



UNIVERSITY OF LEEDS

This is a repository copy of *Process-Focused Synthesis, Crystallization, and Physicochemical Characterization of Sodium Lauroyl Isethionate*.

White Rose Research Online URL for this paper:
<http://eprints.whiterose.ac.uk/128372/>

Version: Accepted Version

Article:

Jeraal, MI, Roberts, KJ orcid.org/0000-0002-1070-7435, McRobbie, I et al. (1 more author) (2018) *Process-Focused Synthesis, Crystallization, and Physicochemical Characterization of Sodium Lauroyl Isethionate*. *ACS Sustainable Chemistry and Engineering*, 6 (2). pp. 2667-2675.

<https://doi.org/10.1021/acssuschemeng.7b04237>

© 2017 American Chemical Society. This document is the Accepted Manuscript version of a Published Work that appeared in final form in *ACS Sustainable Chemistry and Engineering*. © American Chemical Society after peer review and technical editing by the publisher. To access the final edited and published work see <https://doi.org/10.1021/acssuschemeng.7b04237>.

Reuse

Items deposited in White Rose Research Online are protected by copyright, with all rights reserved unless indicated otherwise. They may be downloaded and/or printed for private study, or other acts as permitted by national copyright laws. The publisher or other rights holders may allow further reproduction and re-use of the full text version. This is indicated by the licence information on the White Rose Research Online record for the item.

Takedown

If you consider content in White Rose Research Online to be in breach of UK law, please notify us by emailing eprints@whiterose.ac.uk including the URL of the record and the reason for the withdrawal request.



eprints@whiterose.ac.uk
<https://eprints.whiterose.ac.uk/>

A Process Focused Synthesis, Crystallization and Physicochemical Characterization of Sodium Lauroyl Isethionate

Mohammed I. Jeraal^{1}, Kevin J. Roberts¹, Ian McRobbie² and David Harbottle¹*

1) School of Chemical and Process Engineering, University of Leeds, Woodhouse Lane, Leeds, LS2 9JT, UK

2) Innospec Ltd, Innospec Manufacturing Park, Oil Sites Road, Ellesmere Port, CH65 4EY, UK

**email: cm09mij@leeds.ac.uk*

Abstract

There is a notable lack of published data concerning sodium cocoyl isethionate (SCI) despite widespread application in the personal care industry. A specific homologue, sodium lauroyl isethionate (SLI) was therefore synthesized, purified by recrystallization and then subjected to a detailed physicochemical examination. Purity of 98% was achieved via repeat recrystallization in methanol. A turbidimetric solubility analysis was then executed to identify both its crystallizability and metastable zone width as a function of temperature. Thermogravimetric analysis yielded decomposition onsets of 330°C for the purified SLI. A dynamic vapor sorption study also demonstrated reversibility in the 2.3% mass gained, when exposed to sustained humidity of 87%. Surface tension measurements of purified SLI yielded a critical micellar concentration (CMC) of 5.4 mM and a plateau surface tension of 38 mN/m at 20°C. Both values were lower than the previously reported values for SLI in water, thus indicating the performance benefits of purified isethionates in personal care formulations. The single step synthesis was chlorine-, catalyst- and solvent-free, thus improving process efficiency, safety and throughput over existing SLI syntheses. The succeeding physicochemical analysis crucially provides a much needed insight into the purification, properties and performance of isethionate ester surfactants; all of which is strongly applicable to their commercial manufacture from biorenewable sources.

Keywords

Surfactant, Recrystallization, Surface-tension, Dynamic vapor sorption, Calorimetry, Solubility.

Introduction

Personal care products such as soap bars, shampoos and liquid cleansers contain surfactants to remove grease and sebaceous oils from the skin. Repeated exposure to surfactants is known to cause skin irritation,¹ dryness,² tightness³ and damage to the stratum corneum.⁴ These effects are reported with the use of both traditional carboxylate soaps and synthetic surfactants such as sodium dodecyl sulphate (SDS).⁵⁻⁹ Sodium cocoyl isethionate (SCI) is a milder surfactant also prevalent in personal care formulations.¹⁰ Its lower charge density, larger polar head group and high activity at neutral pH improves its compatibility with the skin, thus reducing the negative effects experienced by the consumer.⁸ Studies have demonstrated reduced irritation,⁸ dryness¹¹ and binding to the stratum corneum,¹² compared with soaps and alkyl sulphates. In the presence of hard water, traditionally saponified carboxylate soaps exhibit a loss in surface activity as the sodium counter-ion is displaced by magnesium and calcium ions.¹³ A larger quantity of product is often utilised by consumers in order to compensate for the consequent loss in detergency and lather.¹⁴ The poor aqueous solubility of the inactive alkali earth salts also results in the precipitation of solid ‘scum’ on bathroom surfaces.¹⁵ SCI is conversely stable in the presence of alkali earth metals and does not form any deposits or display significant loss of lather volume in the presence of hard water.^{14, 16}

The molecular structure of SCI is shown in Fig. 1. On a commercial scale SCI is manufactured through the functionalisation of hydrolyzed coconut oil.¹³ Once hydrolyzed, the coconut oil consists of a blend of linear, saturated carboxylic acids ranging between octanoic (C8) and octadecanoic acid (C18). Sodium derivatives are most prevalent within surface active isethionates; although protic¹⁷ and ammonium¹⁸ isethionates have also been prepared for pharmaceutical applications.

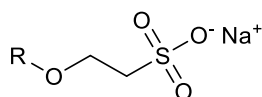


Figure 1. Molecular structure of the isethionate functional group. In sodium cocoyl isethionate (SCI), R = linear, saturated carboxylic acid chain between octanoyl- (C8) and octadecanoyl- (C18).

A compositional analysis of coconut oil indicates that the dodecanoyl (C12), tetradecanoyl (C14) and octadecanoyl (C18) chain lengths are the most abundant with concentrations of 47.7%, 19.9% and 10.3% respectively.¹⁹ Although this chain length distribution is representative of commercial SCI, there is a natural disparity between batches due to the compositional variation in the raw material.¹⁴ Because of this variation, previous studies on SCI have focused on the most abundant isethionate derivatives existing in the natural surfactant blend.

Bistline et al. prepared a series of even numbered, consecutive isethionates ranging from sodium dodecanoyl isethionate (C12) to sodium octadecanoyl isethionate (C18) via a two-step catalytic process.²⁰ The corresponding linear, saturated carboxylic acids were first esterified using propyne under zinc catalysis to form the equivalent isopropenyl esters. These derivatives were then mixed with sodium isethionate and heated to 200°C in the presence of *p*-Toluenesulfonic acid to create the desired acyl isethionate.²⁰ Hikota also prepared sodium decanoyl isethionate (C10) and sodium dodecanoyl isethionate (C12) as part of a larger investigation into ester-based surfactants.²¹ Carboxylic acids were reacted with thionyl chloride to form the corresponding acyl chlorides. Following a reduced pressure distillation, the acyl chlorides were reacted with sodium isethionate at 90°C to yield the acyl isethionate surfactants. Both studies utilised a two-step synthesis route and while Hikota's reaction temperature was lower, the chlorinated reagents were significantly more hazardous than those utilised by Bistline et al.²⁰ In the aforementioned studies, both authors repeatedly recrystallized the sample in alcoholic solvent to purify the crude product. A recent review of acyl isethionates,²² reports that commercially synthesized SCI typically ranges in crude purity from 78 to 85% and the product is not purified prior to application in personal care formulations.¹³

In the current study, sodium lauroyl isethionate (SLI), the most abundant constituent in the natural SCI blend, has been synthesised via the single-step esterification of lauric acid and sodium isethionate. Our reaction exhibits numerous environmental advantages over previous studies reporting the synthesis of SLI including a reduced number of reaction steps, an

increased atom economy and complete removal of solvent, catalyst and chlorinated species from the synthesis.

Following synthesis, the crude SLI was successively recrystallized in methanol with accompanying purity analyses at each stage. A polythermal solubility turbidimetric analysis was subsequently completed to determine the optimum crystallization parameters for the scalable purification of SLI. There is a notable lack of published literature concerning the fundamental properties and characteristics of sodium acyl isethionates. The resultant purified surfactant was therefore subjected to a detailed physicochemical characterisation and analysis which included melting, decomposition, vapor sorption and surface tension measurements. The fundamental data reported in the study provides a much needed insight into how the physicochemical properties influence the commercial scale manufacture, performance and synthesis of acyl isethionate surfactants from biorenewable sources.

Materials and Experimental Methods

Materials. *Synthesis and purification of sodium lauroyl isethionate.* Lauric acid (99%, Acros Organics) and sodium isethionate (98%, Acros Organics) were obtained from Fisher Scientific. Methanol (99.8%) was obtained from VWR. Materials were used as supplied with no further purification. *Cationic titration for surfactant activity.* Methylene blue (96%, Alfa Aesar), anhydrous sodium sulphate (99%, Fisher Scientific), sulphuric acid (95-98%, Sigma Aldrich), dichloromethane (99.8%, VWR) and Hyamine® 1622 (0.004 M, Sigma Aldrich) were used as received.

Synthesis of sodium lauroyl isethionate. 150 g of lauric acid and 85 g of sodium isethionate were placed in a 500 mL three necked round bottom flask and flushed with nitrogen for 20 min. The materials were heated to 60°C under a continuous nitrogen stream while the dispersion was stirred at 600 rpm using a magnetic stirrer. Once the lauric acid had melted the reaction temperature was incrementally increased to 240°C over 1 h. Distilled lauric acid was returned to the reaction flask via a Dean-Stark receiver while the water of reaction, along with any biphasic interfacial material, was retained within the receiver and removed as necessary. After 4 h, the Dean-Stark apparatus was removed and replaced with a vertical still head coupled with a 250 mL two neck receiving flask. Nitrogen flow was momentarily increased to minimise hydrolysis during equipment exchange. A condenser was fitted to the receiving flask and the unreacted lauric acid was collected via vacuum distillation. The vacuum pressure was regulated

using nitrogen to reduce foaming and product degradation. Crude SLI was isolated by pouring the molten liquid onto a glass surface. Purity was determined by cationic titration with benzethonium chloride (Hyamine® 1622), as reported by Longman.²³

Recrystallization of sodium lauroyl isethionate. The crude SLI was purified by repeat recrystallization in methanol. SLI was mixed with 100 mL of methanol and heated to 60°C in a round bottom flask with a condenser. The mixture was stirred at 300 rpm with the solvent incrementally added until the SLI had completely dissolved. Any insoluble particles observed in solution were hot filtered through a stemless funnel. Solutions were then cooled overnight at 0.5°C/min. The resulting crystals were isolated via Buchner filtration and dried in a vacuum desiccator prior to further purification steps. Cationic benzethonium chloride titrations were completed at each purification step, as previously described. After five recrystallizations, SLI was obtained in the form of white powder. The purified material was used for the subsequent physicochemical analysis. NMR, FTIR and LC-MS data of the crude and purified SLI is provided in the ESI Sec. 3.2.

Thermal analysis of sodium lauroyl isethionate. Thermogravimetry. Samples of lauric acid, crude SLI and purified SLI were analysed using a Mettler Toledo TGA/DSC 1 Thermogravimetric Analyser. 2-5 mg of each sample was weighed to the nearest 0.1 µg using a Mettler Toledo UMX2 Ultra-Microbalance and placed in a 70 µL alumina crucible. Samples were heated from 25°C to 500°C at 10°C/min under a N₂ flow of 50 mL/min. Sample mass was measured every second to the nearest 0.01 µg to identify any temperature induced phase transitions. The analysis was used to determine the presence of ancillary species of the crude and purified samples of SLI. *Differential scanning calorimetry.* Samples of crude SLI and purified SLI were analysed using a Mettler Toledo DSC 1. 2-5 mg of each sample was weighed and deposited in hermetically sealed 40 µL aluminium crucibles. Samples were heated from 25°C to 150°C at 50°C/min under a N₂ flow of 50 mL/min. After 10 min at 150°C, the temperature was raised by 1°C/min to 250°C. Following a further 10 min, the temperature profile was reversed and the temperature reduced to 25°C at 1°C/min. Prior to analysis, the instrument was calibrated against certified reference materials of zinc and indium obtained from Mettler Toledo. Enthalpy of fusion (ΔH_{Fus}) and melting temperature (T_m) were obtained from the area and the peak maximum temperature observed from the primary melting peak.

Dynamic vapor sorption. The water vapor sorption of purified SLI was measured using the DVS Advantage (Surface Measurement Systems, UK). Approximately 10 mg of sample was

added to an aluminium crucible and placed into a thermostatically controlled chamber at 25°C. Samples were then dried under a flow of dry N₂ at 50 mL/min until the sample mass had stabilised to the nearest 0.1 µg over a period of 5 min. Relative humidity (RH) was subsequently varied between 0 and 90%, at 10% increments. Target humidity levels were maintained until the sample mass had stabilized and the sample mass, humidity and temperature were continuously recorded at 60 s intervals. The data provides information on the storage stability of SLI with respect to changing humidity levels at room temperature.

Solubility. Solutions of SLI in methanol were prepared at concentrations between 20 g/L and 35 g/L, at 5 g/L increments. Purified SLI was accurately weighed using an analytical balance (to the nearest 0.1 mg) and diluted with 5 mL methanol. The resulting solutions were heated to 40°C and stirred at 300 rpm to ensure complete dissolution. Micropipettes were then used to transfer 1 mL of each solution into 1.5 mL capped glass vials. Four vials were filled at each concentration, thus 16 samples were considered for further analysis. The solutions were analysed using the Technobis Crystal16 parallel crystallizer. The crystallizer provides independent temperature control of four blocks, with each block consisting of four glass vials. Samples were subjected to five heating and cooling cycles between -10 to 50°C, with each solution concentration undergoing rates of 3, 2, 1 and 0.5 °C/min. Vials were individually magnetically stirred at 700 rpm and solubility was determined using the integrated turbidity detectors. T_{Diss} (clear point) was identified as the temperature when the measured transmission equalled 100% during heating, while T_{Cryst} (cloud point) was identified as the temperature when the transmission first dropped below 95% upon cooling. Sample vials were continuously flushed with N₂ to avoid external surface condensation at low temperatures. Equilibrium solubility parameters at each concentration (T_{Diss} and T_{Cryst}) were obtained by plotting the respective values against heating rate and extrapolating to 0°C/min. The experimental solubility was then compared with the ideal solubility through a Van't Hoff analysis.

Praustnitz et al.²⁴ stated that, assuming a negligible contribution from the heat capacity (C_p), the molar solubility (χ) in an ideal system was obtained from eq. (1) using the enthalpy of fusion (ΔH_{Fus}) and melting temperature (T_m) measured via DSC:

$$\ln(\chi) = \frac{\Delta H_{Fus}}{R} \left[\frac{1}{T} - \frac{1}{T_m} \right] \quad (1)$$

The enthalpy and entropy of dissolution (ΔH_{Diss} and ΔS_{Diss} respectively) were then calculated from the ideal and experimental solubility data using eq. (2). These values quantify the enthalpy change when one mole of solute is dissolved into an infinite quantity of saturated solution.

$$\ln(\chi) = -\frac{\Delta H_{Diss}}{RT} + \frac{\Delta S_{Diss}}{R} \quad (2)$$

The activity co-efficient (γ) was then used to quantify the experimental deviation from ideality, in accordance with eq. (3), where χ and χ_{Ideal} are the experimental and ideal molar solubilities.

$$\gamma = \frac{\chi_{Ideal}}{\chi} \quad (3)$$

Further details on the experimental method and subsequent analysis can be found in previous publications.^{25 26}

Surface tension. Solutions of SLI in water were prepared at concentrations between 0.01 mM and 10 mM as described previously. A single droplet was generated at the tip of a blunt-end 22 gauge needle with a 1 mL Hamilton 1001 LT threaded syringe. Surface tension was measured using a Theta tensiometer (Biolin Scientific) in the pendant drop mode. A period of 10 min (frame rate capture, 1 fps) was allocated to stabilize the droplet and ensure accurate measurement of the surface tension. Edge detection was applied to the images and the droplet shape was fitted to the Young-Laplace equation using the Attension Theta software. The equilibrium surface tension was determined by averaging the last 30 images of the 10 min period, with three experimental repeats at each concentration. The needles were replaced between samples and the syringes were rinsed with deionised water and oven dried before reuse. All sample preparation and measurements were obtained at room temperature, 20°C. Surface tension of the air-water interface was measured to be 72.7 ± 0.1 mN/m.

Results and Discussion

A compositional analysis of a commercial hydrolysed coconut oil blend, typically used to synthesize SCI, is displayed in Fig. 2. The fatty acid mixture was derivatized to form the corresponding fatty acid methyl esters (FAMES) to avoid peak tailing and long retention times. The resulting GC-MS chromatogram correlates with the review literature,¹⁹ indicating that the dodecanyl (C12), tetradecanyl (C14) and octadecanyl (C18) are the most abundant chain lengths with concentrations of 43.9%, 20.0% and 10.9%, respectively. Due to the abundance

of the dodecyl chain length in the commercial feedstock, the lauryl (C12) homologue of SCI, sodium lauroyl isethionate (SLI), was selected as a model isethionate ester surfactant for this study.

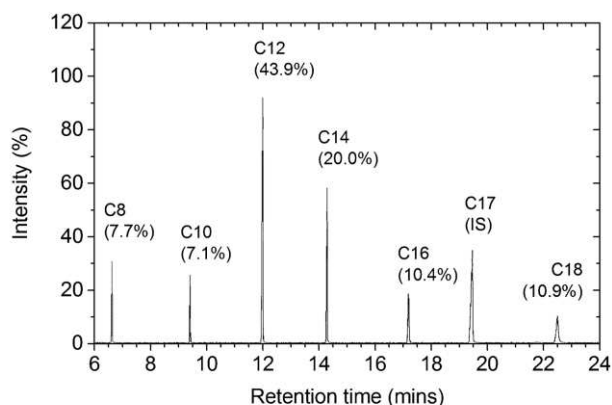


Figure 2. Gas chromatogram depicting the chain length distribution of carboxylic acids within the coconut derived fatty acid blend used to commercially synthesize sodium cocoyl isethionate. Analyzed as FAMES via GC-MS. See ESI Sec. 1.1 for derivatization and analytical procedure.

Synthesis and purification of SLI. Sodium lauryl isethionate (SLI) was synthesised via a single-step esterification of lauric acid and sodium isethionate under solvent- and catalyst-free conditions. During the commercial synthesis of similar amide-based surfactants, a continuous recycle of distilled volatile carboxylic acids has been incorporated to maintain the acid excess necessary to drive the acylation.²⁷ In the synthesis of isethionates from biorenewable sources, the recycle of volatile components ensured that the desired chain length distribution of the feed material was maintained in the product. The distillation of fatty acids of a controlled composition also means these raw materials can be reutilised in future syntheses with minimal change to the physical properties of the resulting product.

In the current study, SLI was obtained at a crude purity of 83% (via cationic titration) following a vacuum distillation. This purity is comparable to analogous materials produced via alternative synthesis routes which include catalysts and solvents, where the highest reported purity was 85%.²² Successive cooling crystallizations in methanol at 0.5°C/min led to a 15% increase in

purity following three purification cycles, after which no significant improvement was observed (Fig. 3).

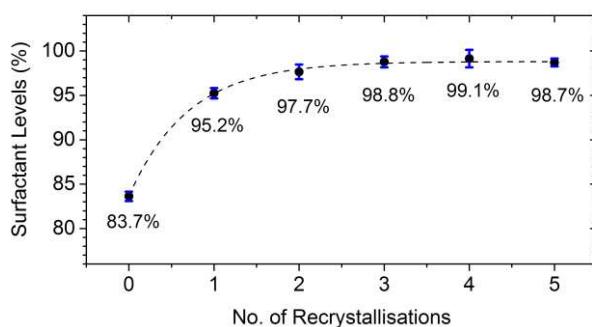


Figure 3. Purification profile of the SLI product. Repeat cooling crystallizations were conducted from 60°C to 20°C at 0.5°C/min. Surfactant levels were measured at each stage via cationic titration with benzethonium chloride. Data was fitted to an exponential association function.

As alkaline potentiometric pH titrations fail to distinguish between the surfactant and residual acid,²⁸ the industry standard method of cationic titration with benzethonium chloride solution was used for determining surfactant levels. However, this method has been reported to display an error of ~1%, as observed in the current study.²⁸ Possible attributable phenomena include operator error, the sparing solubility of organic complexes in the aqueous phase, and trace inorganic impurities in the methylene-blue solution.²³ Although newer titrants such as dialkylmethylimidazolium chloride (TEGO®trant) address some of these discrepancies,²⁹ an LC-MS analysis was additionally utilised in the current study to confirm that a purity of 98% had been achieved after three purification steps. Chemical structure was further verified by NMR, see ESI Fig. S6 for analytical data.

Thermal analysis of SLI. Thermogravimetric analysis of the crude and purified samples (Fig. 4) confirms that the main impurity within the crude SLI was residual lauric acid, which was removed to undetectable quantities in the purified sample. The absence of a measureable mass loss below 300°C in the purified SLI indicates that the anhydrous form of the surfactant was obtained and the subsequent storage of the purified SLI at an ambient humidity of ~60% for several weeks resulted in no significant moisture uptake. From an average of three measurements, the decomposition onset temperature of purified SLI was determined to be $331 \pm 1^\circ\text{C}$. Consequently, there is minimal risk of thermal decomposition (and formation of SO_2 and SO_3) at the proposed reaction temperature of 240°C.

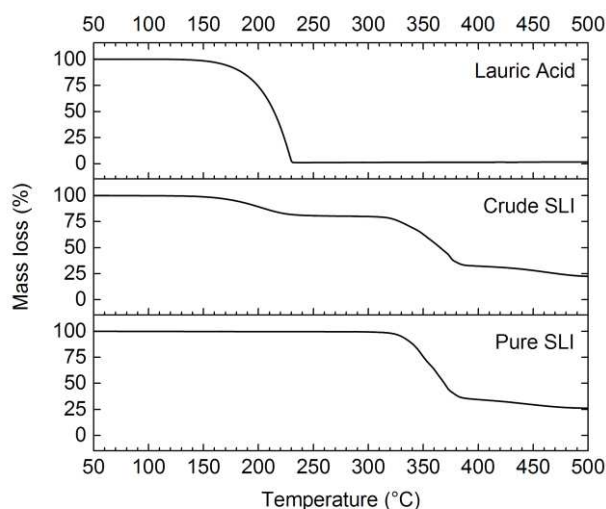


Figure 4. TGA profiles of lauric acid, crude and purified SLI at a heating rate of 10°C/min. Mass loss was normalised as a percentage of the initial sample mass. As used to identify the presence of moisture at 100°C, impurities between 150 and 230°C and the decomposition profile of SLI in excess of 300°C.

Differential scanning calorimetry (DSC) of the purified SLI (98% purity) produced a peak melting temperature of 225.2°C with a melting range of 224-226°C, see Fig. 5. The previously reported melting range for SLI was 214-216°C, but no quantified purity was specified.²⁰ The crude SLI (melting temperature of 214.2°C) displayed some correlation with the previously reported values, thus suggesting that an improved purity could be the cause of the disparity with previous data through freezing point depression. The peak broadening observed in the crude SLI are suspected to result from combinations of the lauric acid and sodium isethionate pre-cursors.

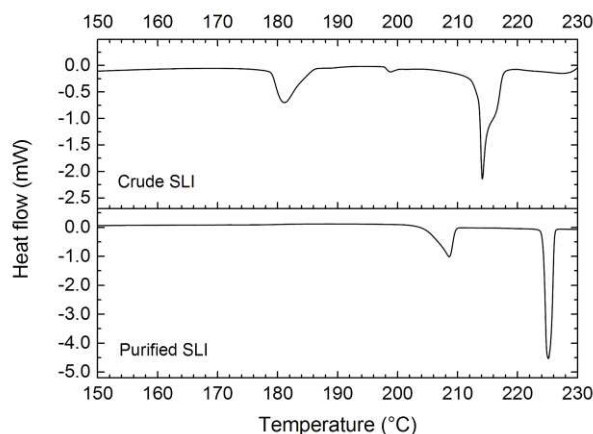


Figure 5. DSC analysis of crude reaction SLI and purified SLI. Samples were heated to 150°C at 50°C/min and then heated to 250°C at 1°C/min. Crude and purified SLI exhibited peak melting temperatures of 214.2°C and 225.2°C, respectively.

Measuring five independent SLI samples, the corresponding melting enthalpy (ΔH_{Fus}) was found to be 162 ± 2 kJ/mol. The transition at $\sim 210^\circ\text{C}$ in the purified SLI and $\sim 180^\circ\text{C}$ in the crude SLI are believed to be thermotropic phase transitions. These are widely reported to exist in many long chain anionic surfactant systems in the absence of water.³⁰⁻³²

Dynamic vapor sorption analysis of SLI. An isothermal DVS analysis was conducted at 25°C to better understand moisture uptake during the commercial storage of isethionate ester surfactants. Although Karl-Fischer titration is the most common method of determining bulk moisture content in anionic surfactants,²⁸ the DVS method can provide sorption kinetics and thermodynamic data over a range of humidity levels.^{33,34} Prior to measurement, sample drying under N₂ flow showed a total mass loss of 0.01%. While alkyl sulfates are known to readily exist in hydrate form,³⁵⁻³⁷ the lack of significant moisture loss observed during TGA and DVS analyses suggests that the anhydrous form of SLI was obtained using the current synthesis method. At 40% R_H the sample mass had increased by 0.2%, suggesting relative stability of the sample during storage at or below 40% R_H. At 87% R_H, the mass gain was 2.35% which confirms the surfactant to be “slightly hygroscopic” according to Callahan et al.³⁸ and the European Pharmacopoeia.³⁹ There are three primary sorption mechanisms by which materials take up moisture: i) surface adsorption, ii) bulk adsorption and iii) liquefaction by surface dissolution.⁴⁰ On reducing the R_H to 0% the sample mass returned to its original value with an insignificant discrepancy of 0.005%. Since the sorption process is reversible, liquefaction is unlikely to be the predominant mechanism. With a 2.35% mass increase at 87% R_H, the

surfactant could have formed a hemihydrate, which would yield a theoretical mass increase of 2.7%. Further analysis would be required to confirm both the structure and mechanism pertaining to the proposed transition. The hysteresis shown in Fig. 6 does however indicate that any moisture uptake during storage at higher humidity can be significantly reduced if the sample is later exposed to a humidity level below 20%. This irreversibility is common in the sorption analysis of solid-gas systems.⁴¹ While the hysteresis is significantly reduced below 20% RH, hysteresis is observed to some extent across the entire humidity range. Everett suggests that this behaviour results from a sorption mechanism that is independent of solid surface area,⁴² thus supporting the postulation of a molecular hemihydrate species at elevated humidity levels.

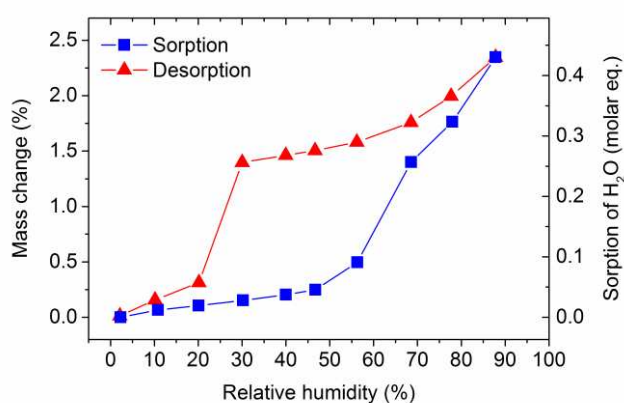


Figure 6. Dynamic vapor sorption analysis of purified SLI. The technique determines hygroscopicity by adjusting humidity levels and measuring the resulting sample mass. SLI was exposed to relative humidity levels between 0 and 90%, resulting in both sorption and desorption isotherms at a thermostatically controlled temperature of 25°C. Left axis shows mass increase relative to the initial mass of SLI (%). Right axis displays this increase as the molar sorption of water, relative to one mole of SLI. Full time-resolved data for purified SLI is provided in ESI Sec. 5, Fig. S13.

Crystallizability of SLI. A polythermal solubility analysis was conducted to define the optimal crystallization parameters for the commercial purification of isethionate surfactants. This approach was utilised in the current study as there was no prior solubility data for the SLI sample. Alcoholic solvents were considered as the purification solvent for SLI after a recent study revealed them to exhibit a high solubility for lauric acid, which the TGA data indicated to be the primary impurity in the crude product. Methanol was specifically selected as it exhibits a higher solubility for lauric acid than ethanol,⁴³ isopropanol⁴⁴ and n-butanol⁴⁴ at 20°C.

Preliminary solubility studies yielded very high ambient solubility in water, while ethanol exhibited a significantly lower solubility than methanol at elevated temperatures. Although methanol exhibits a higher toxicity than these substances, the preliminary data indicates that their adoption would be detrimental to both throughput and recoverable yields of SLI. Methanol was selected in preference to maximize the corresponding commercial value of the purification process.

Fig. 7a shows the turbidimetric data for purified SLI in methanol during a heating and cooling cycle, highlighting well defined crystallization and dissolution on-set points as a function of temperature. The TGA, NMR and LC-MS analyses of the recrystallized SLI confirmed that the resulting precipitate was free from significant solvent and impurity levels. The metastable zone width (MSZW) as a function of cooling rate, displayed in Fig. 7b, shows how equilibrium crystallization and dissolution temperatures (T_{Cryst} and T_{Diss}) were explained. The MSZWs, as well as T_{Cryst} and T_{Diss} , were collated at each concentration to form the solubility curve of SLI in methanol (Fig. 7c).

The metastable zone denotes conditions where the system is beyond the solubility limit and nucleation can be induced through seeding, surface coarseness or the presence of foreign particulates.⁴⁵ Spontaneous nucleation in a binary homogenous system is kinetically precluded until the system reaches the limit of the metastable zone (Fig. 7c).⁴⁶ The minimal dependence of the MSZW on the cooling rate at 20 g/L (Fig. 7b) is reflected for all solution concentrations, see ESI Fig. S11. This phenomenon indicates the crystallisation and dissolution kinetics are not rate limiting to their respective phase transition processes.²⁶ With decreasing temperature the system exhibits an increasing MSZW. Knowledge of these changes to MSZW are important to controlling the commercial crystallisation processes and thus ensuring a reproducible crystal size, morphology and purity between batches.⁴⁵ The implementation of *in-situ* process analytical techniques could be used to maintain process conditions within the metastable zone at high temperatures, where the MSZW is smaller.⁴⁷

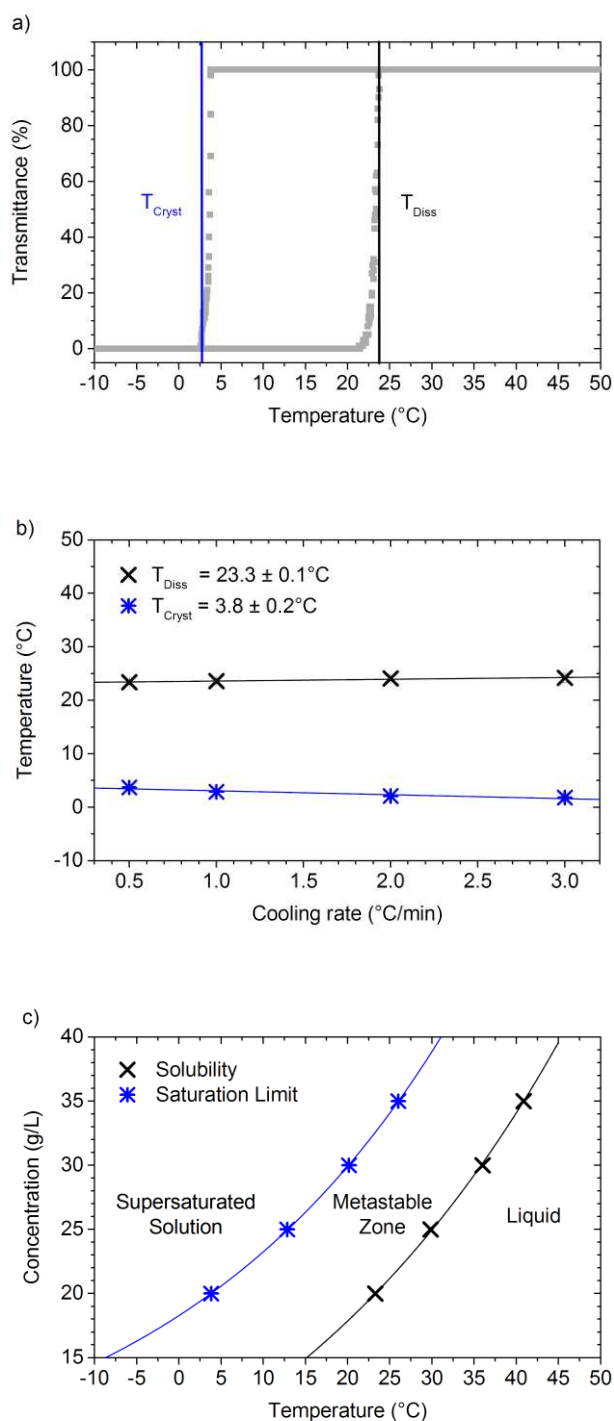


Figure 7. Polythermal turbidimetric solubility analysis of purified SLI in methanol between -10°C and 50°C at 700 rpm. a) Reaction profile of light transmission (%) vs. temperature ($^\circ\text{C}$) depicting the extraction of crystallization (T_{Cryst}) and dissolution (T_{Diss}) temperatures from Crystall16 system at 20 g/L. b) Change in T_{Cryst} and T_{Diss} with varying cooling rates at 20 g/L. Extrapolation to $0^\circ\text{C}/\text{min}$ provides equilibrium values of T_{Cryst} and T_{Diss} . Legend displays equilibrium transition temperatures with the linear regression error. c) Solubility curve of purified SLI in methanol plotted from equilibrium transition temperatures (T_{Cryst} and T_{Diss})

at all studied concentrations. Crystallization and dissolution events were measured at concentrations of 20, 25, 30 and 35 g/L, each at temperature ramps of 3, 2, 1 and 0.5°C/min. See Figure S9 and S10 in the ESI for turbidimetric profiles and solubility data of all concentrations and cooling rates.

Solubility Analysis of SLI. Through a van't Hoff analysis, the experimental solubility data can be compared with the ideal solubility of SLI, in a solvent-free environment, to determine the influence of the solvent on the crystallization behavior. Both ideal and experimental Hoff analyses of SLI are shown in Fig. 8. The temperature dependent activity coefficient (γ) for the crystallization of SLI in methanol was calculated to quantify the deviation from ideality induced by the methanolic solvent environment. See Table 1. Full data can be found in the ESI Fig. S11. This large deviation from ideality, when compared to other organic systems analysed using the same methodology,²⁶ suggests that the solvent-solute system exhibits a strong preference for solute-solute interactions. When the data is compared with a conductivity-based solubility analysis of SDS, the solubility of SLI in methanol at 50°C is approximately ~30% of the measured SDS solubility.⁴⁸ With respect to theoretical yields, a cooling crystallization from -10°C to 50°C is predicted to recover more SLI than SDS, with predicted yields of 79% and ~71% respectively. The values of ΔH_{Diss} and ΔS_{Diss} for SLI indicate that the phase transition is strongly dependent on the enthalpy, see Table 1. The thermodynamic parameters for the dissolution of SDS in methanol are $\Delta H_{\text{Diss}} = 22.3 \text{ kJ mol}^{-1}$ and $\Delta S_{\text{Diss}} = 54.3 \text{ J mol}^{-1}$.⁴⁸ Despite analogous dodecyl alkyl chains, the additional ethyl-ester group in the isethionate species creates a difference in chain length between SDS and SLI. This structural disparity and consequent hydrophilicity may contribute to the higher absolute solubility exhibited by SDS in a methanolic environment.

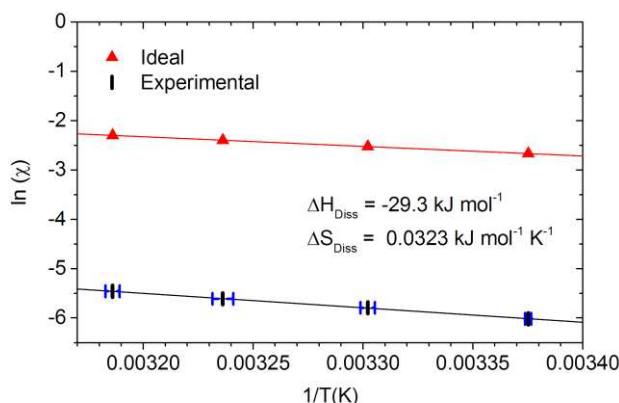


Figure 8. van't Hoff plot of polythermal solubility analysis of purified SLI in methanol between -10°C and 50°C . χ = mole fraction of SLI in methanol. Ideal solubility was calculated from the melting enthalpy (ΔH_{Fus}) and temperature (T_{Fus}) obtained via DSC. Activity coefficients measuring deviation from ideality is displayed Table 1, with full details in the ESI Fig. S11.

Surface tension measurements of aqueous SLI solutions. The CMC of SLI at 20°C was found to be 5.36 mM with a lower plateau surface tension of 37.9 mN/m, see Fig. 9. Bistline et al. reported a slightly higher CMC (6.4 mM) and plateau surface tension (46.6 mN/m) for SLI synthesized by the two-step process.²⁰ The lower surface tension in the current study suggests a higher wettability in aqueous environments, while a lower CMC confirms that a lower surfactant concentration was required to reach peak wetting performance. It is worth noting that the method used to determine the CMC and surface tensions was different from that reported by Bistline et al.²⁰ However, the observed improvement in performance is more likely to result from an improved sample purity, as the CMC of lauryl sulphate surfactants is very susceptible to error from surface active impurities.⁴⁹ Foreign species can cause the surface tension to fluctuate and drop, below the CMC limit before stabilising at the actual micellar concentration.⁵⁰ The absence of such fluctuation provides evidence that such impurities were not present in the current sample.

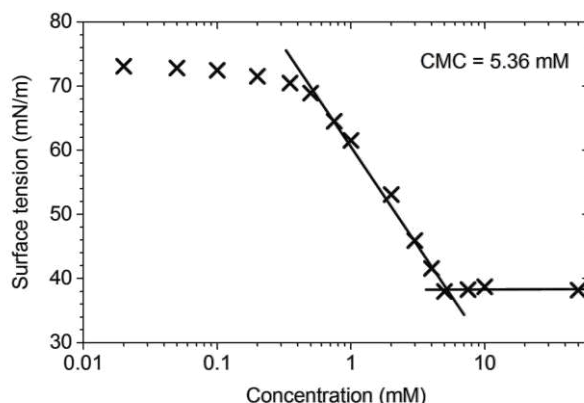


Figure 9. Surface tension as a function of the SLI concentration in water. The surface tension was determined by pendant drop analysis at 20°C. Equilibrium surface tension values were obtained by fitting the droplet shape to the Young-Laplace equation. Reported values are an average of 30 consecutive images (1 fps).

Recent studies have shown that SDS exhibits a CMC of 8.0 mM at 20°C,⁵¹ with a corresponding plateau surface tension of 33 mN/m at pH 7.⁵² The plateau surface tension beyond the CMC for SLI (38 mN/m) is therefore lower than that measured for SDS (33 mN/m) at 20°C. The CMC, however, for SLI is higher than that for SDS at equivalent conditions. Hence, the proposed crystallization process and resultant higher sample purity could therefore be critical to obtaining surface tension levels exhibited by SDS whilst maintaining the increased mildness offered by isethionate ester surfactants.

In summary, the thermodynamic and physicochemical properties determined from the characterization of SLI are provided in Table 1, along with the corresponding literature values for its alkyl sulfate analog, sodium dodecyl sulfate (SDS).

Table 1. Thermodynamic and physicochemical properties of purified SLI (current study) and SDS (literature values).

	T_m (°C)	Solubility in MeOH* (g/L)	ΔH_{Diss} in MeOH (kJ mol ⁻¹)	ΔS_{Diss} in MeOH (kJ mol ⁻¹)	Activity coeff. in MeOH* (γ)	CMC* (mM)	Surf. tension at CMC* (mN/m)
SLI	225	17.9	29.3	0.0322	29.1	5.4	37.9
SDS	206 ⁵³	79.1 ⁴⁸	22.3 ^{† 48}	0.0543 ^{† 48}	<i>n/a</i>	8.0 ⁵¹	33 ^{‡ 52}

* Measured at 20°C. ‡ pH 7 † Parameters obtained by processing the cited raw data using methodologies described in the current study.

Conclusions

Sodium lauroyl isethionate (SLI), the most abundant derivative of sodium cocoyl isethionate (SCI), was directly synthesised at the 500 mL scale without the use of solvent or catalytic species. The direct esterification of lauric acid reduced the number of reaction steps and eliminated the risk of HCl production which resulted from previous acyl chloride based reactions.²¹ When compared with current published syntheses of SLI, the solvent-free route was found to have the potential to increase process output, reduce material costs and remove the time and energy required for an industrial scale solvent recovery. While catalytic routes had previously been proposed for this type of reaction,²² their use had led to an undesired phase separation in the resulting product at concentrations above 0.2 w/w%.⁵⁴ The reaction times, temperatures and yields in the current study were also similar to previous catalytic routes.²² The new process therefore eliminated the handling and recovery of catalytic materials without significant detriment to process efficiency.

The proposed recrystallization of crude SLI resulted in a purity level of 98% after three successive recrystallizations in methanol. Following a recent review of commercially available surfactants,²² this is considered by the authors to be the highest published purity of a sodium acyl isethionate surfactant. The use of crystallization over chromatographic techniques meant that the purification could be scaled to industrial quantities and the solubility analysis of the purified surfactant provided process conditions through which this could be achieved. Although this study utilized a cooling crystallization, the data was also deemed applicable to

evaporative processes.⁵⁵ While the estimated throughput was lower than an analogous purification of SDS, SLI displayed higher yields at equivalent temperatures which was prospectively more important given its higher market value.

An aqueous surface activity analysis of the purified SLI yielded a surface tension much closer to the performance of SDS than previously reported synthesised samples of SLI. Given the widely acknowledged mildness of isethionate ester surfactants compared to traditional soaps and synthetic surfactants such as sodium dodecyl sulfate (SDS), the increased performance achieved through purification could be utilised in high value personal care formulations where harsher surfactants may be undesirable. High purity isethionates could also be used to create analytical standards, thus permitting the adoption of spectroscopic techniques to evaluate commercial surfactant synthesis. Reductions in time, labor and chemical use could be achieved when compared with the successive titration techniques currently used to detect and quantify surfactants in the personal care industry.

List of Abbreviations

CMC – critical micellar concentration
DSC – differential scanning calorimetry
DVS – dynamic vapor sorption (relates specifically to dynamic water vapor sorption in the current study)
FAME – fatty acid methyl ester
MSZW – metastable zone width
SCI – sodium cocoyl isethionate
SDS – sodium dodecyl sulfate
SLI – sodium lauroyl isethionate
TGA – thermogravimetric analysis
 ΔH_{Diss} – enthalpy of dissolution
 ΔH_{Fus} – enthalpy of fusion
 ΔS_{Diss} – entropy of dissolution
 T_{Cryst} – crystallization temperature
 T_{Diss} –melting temperature
 T_{m} – melting temperature
 γ – activity co-efficient
 χ – mole fraction

Acknowledgements

We would like to thank the EPSRC Centre for Doctoral Training in Complex Particulate Products and Processes which partially funds the doctoral research of MJ, as well as Innospec

Ltd for their financial support in the completion of this research. We also thank Martin Huscroft and Simon Barrett for analytical support.

Supporting Information

Contains analytical data relating to the purity of SLI including FTIR, LC-MS and NMR. Further results from the titration and DVS experiments are provided, along with experimental details of the FAME derivatization and the titration procedures. Plots of raw turbidimetric data, MSZW determination and activity co-efficient have also been made available.

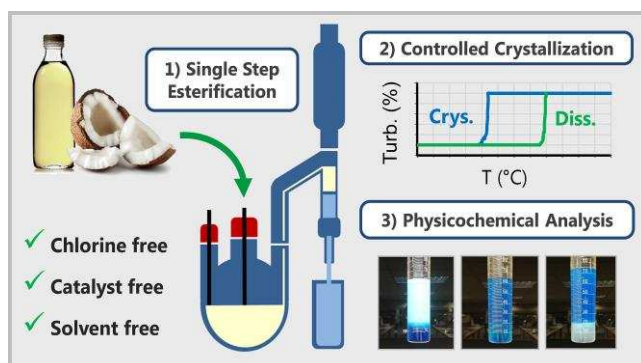
References

1. Froebe, C. L.; Simion, F. A.; Rhein, L. D.; Cagan, R. H.; Kligman, A., Stratum corneum Lipid Removal by Surfactants: Relation to in vivo Irritation. *Dermatology* **1990**, 181 (4), 277-283.
2. Imokawa, G.; Akasaki, S.; Minematsu, Y.; Kawai, M., Importance of intercellular lipids in water-retention properties of the stratum corneum: induction and recovery study of surfactant dry skin. *Arch. Dermatol. Res.* **1989**, 281 (1), 45-51.
3. Kawai, M.; Imokawa, G., The induction of skin tightness by surfactants. *J. Soc. Cosmet. Chem.* **1984**, 35, 147-156.
4. Faucher, J.; Goddard, E., Interaction of keratinous substrates with sodium lauryl sulfate: I. Sorption. *J. Soc. Cosmet. Chem.* **1978**, 29, 323-337.
5. Prottey, C.; Ferguson, T., Factors which determine the skin irritation potential of soaps and detergents. *J. Soc. Cosmet. Chem.* **1975**, 26 (1), 29-46.
6. Sauermann, G.; Doerschner, A.; Hoppe, U.; Wittern, P., Comparative-Study of Skin Care Efficacy and In-Use Properties of Soap and Surfactant Bars. *J. Soc. Cosmet. Chem.* **1986**, 37 (5), 309-327.
7. Strube, D. D.; Nicoll, G., The irritancy of soaps and syndets. *Cutis* **1987**, 39 (6), 544-5, DOI
8. Ananthapadmanabhan, K.; Yang, L.; Vincent, C.; Tsaor, L.; Vetro, K. M.; Foy, V.; Zhang, S.; Ashkenazi, A.; Pashkovski, E.; Subramanian, V., A Novel Technology in Mild and Moisturizing Cleansing Liquids. *Cosmetic Dermatology* **2009**, 22 (6), 307-316.
9. Bárány, E.; Lindberg, M.; Lodén, M., Biophysical characterization of skin damage and recovery after exposure to different surfactants. *Contact Dermatitis* **1999**, 40 (2), 98-103, DOI 10.1111/j.1600-0536.1999.tb05999.x.
10. Petter, P. J., Fatty acid sulfoalkyl amides and esters as cosmetic surfactants. *Int. J. Cosmet. Sci.* **1984**, 6 (5), 249-260, DOI 10.1111/j.1467-2494.1984.tb00382.x.
11. Wilson, D.; Berardesca, E.; Maibach, H. I., In vivo transepidermal water loss and skin surface hydration in assessment of moisturization and soap effects. *Int. J. Cosmet. Sci.* **1988**, 10 (5), 201-211, DOI 10.1111/j.1467-2494.1988.tb00018.x.
12. Ananthapadmanabhan, K.; Yu, K.; Meyers, C.; Aronson, M., Binding of surfactants to stratum corneum. *J. Soc. Cosmet. Chem.* **1996**, 47 (4), 185-200.
13. Friedman, M.; Wolf, R., Chemistry of soaps and detergents: Various types of commercial products and their ingredients. *Clin. Dermatol.* **1996**, 14 (1), 7-13, DOI 10.1016/0738-081x(95)00102-l.
14. Spitz, L., Soap Manufacturing Technology. AOCs Press: Urbana, Illinois, 2010.
15. Soontravanich, S.; Lopez, H. E.; Scamehorn, J. F.; Sabatini, D. A.; Scheuing, D. R., Dissolution Study of Salt of Long Chain Fatty Acids (Soap Scum) in Surfactant Solutions. Part I:

- Equilibrium Dissolution. *J. Surfactants Deterg.* **2010**, 13 (4), 367-372, DOI 10.1007/s11743-010-1208-5.
16. Hollstein, M.; Spitz, L., Manufacture and properties of synthetic toilet soaps. *J Am Oil Chem Soc* **1982**, 59 (10), 442-448, DOI 10.1007/bf02634431.
 17. Western, K. A.; Perera, D. R.; Schultz, M. G., Pentamidine isethionate in the treatment of pneumocystis carinii pneumonia. *Ann. Intern. Med.* **1970**, 73 (5), 695-702, DOI 10.7326/0003-4819-73-5-695.
 18. Barber, H. J.; Slack, R., The search for chemotherapeutic amidines. Part IV. Two polyamidines. *J. Chem. Soc.* **1947**, (0), 82-84, DOI 10.1039/jr9470000082.
 19. Orsavova, J.; Misurcova, L.; Ambrozova, J. V.; Vicha, R.; Mlcek, J., Fatty acids composition of vegetable oils and its contribution to dietary energy intake and dependence of cardiovascular mortality on dietary intake of fatty acids. *Int. J. Mol. Sci* **2015**, 16 (6), 12871-12890.
 20. Bistline, R. G., Jr.; Rothman, E. S.; Serota, S.; Stirton, A. J.; Wrigley, A. N., Surface active agents from isopropenyl esters: Acylation of isethionic acid and N-methyltaurine. *J Am Oil Chem Soc* **1971**, 48 (11), 657-660, DOI 10.1007/bf02638512.
 21. Hikota, T., Studies of Ester-Containing Surfactants. Preparation and Properties of Sodium Sulfoalkyl Alkanoates. *Bull. Chem. Soc. Jpn.* **1970**, 43 (7), 2236-2240, DOI 10.1246/bcsj.43.2236.
 22. Friedman, M., Chemistry, Formulation, and Performance of Syndet and Combo Bars. In *Soap Manufacturing Technology*, Spitz, L., Ed. AOCS Press: Urbana, Illinois, 2016.
 23. Longman, G. F., The analysis of detergents and detergent products. John Wiley & Sons: London (UK), 1976.
 24. Prausnitz, J. M.; Lichtenthaler, R. N.; de Azevedo, E. G., *Molecular Thermodynamics of Fluid-Phase Equilibria*. Prentice Hall: New Jersey (USA), 1998.
 25. Camacho Corzo, D. M.; Borissova, A.; Hammond, R. B.; Kashchiev, D.; Roberts, K. J.; Lewtas, K.; More, I., Nucleation mechanism and kinetics from the analysis of polythermal crystallisation data: methyl stearate from kerosene solutions. *CrystEngComm* **2014**, 16 (6), 974-991, DOI 10.1039/c3ce41098f.
 26. Turner, T. D.; Corzo, D. M. C.; Toroz, D.; Curtis, A.; Dos Santos, M. M.; Hammond, R. B.; Lai, X.; Roberts, K. J., The influence of solution environment on the nucleation kinetics and crystallisability of para-aminobenzoic aci. *Phys. Chem. Chem. Phys.* **2016**, 18 (39), 27507-27520, DOI 10.1039/c6cp04320h.
 27. Sundberg, R. L. Process of preparing ester and amide type anionic surface active agents. 2,857,370, 1958.
 28. Schmitt, T. M., *Analysis of Surfactants*. Marcel Dekker: New York (USA), 2001.
 29. Cui, L.; Puerto, M.; López-Salinas, J. L.; Biswal, S. L.; Hirasaki, G. J., Improved Methylene Blue Two-Phase Titration Method for Determining Cationic Surfactant Concentration in High-Salinity Brine. *Anal. Chem.* **2014**, 86 (22), 11055-11061, DOI 10.1021/ac500767m.
 30. Skoulios, A. E.; Luzzati, V., (FR) La structure des colloïdes d'association. III. Description des phases mésomorphes des savons de sodium purs, rencontrées au-dessus de 100°C. *Acta Crystallogr.* **1961**, 14 (3), 278-286, DOI 10.1107/s0365110x61000863.
 31. Binnemans, K., Ionic Liquid Crystals. *Chem. Rev.* **2005**, 105 (11), 4148-4204, DOI 10.1021/cr0400919.
 32. Klein, R.; Dutton, H.; Diat, O.; Tiddy, G. J. T.; Kunz, W., Thermotropic Phase Behavior of Choline Soaps. *J. Phys. Chem. B* **2011**, 115 (14), 3838-3847, DOI 10.1021/jp2006292.
 33. Gustavsson, C.; Piculell, L., Isotherms and Kinetics of Water Vapor Sorption/Desorption for Surface Films of Polyion-Surfactant Ion Complex Salts. *The Journal of Physical Chemistry B* **2016**, 120 (27), 6778-6790, DOI 10.1021/acs.jpcc.6b02983.
 34. Ouyang, J.; Wang, J.; Wang, Y.; Yin, Q.; Hao, H., Thermodynamic study on dynamic water and organic vapor sorption on amorphous valnemulin hydrochloride. *Frontiers of Chemical Science and Engineering* **2015**, 9 (1), 94-104, DOI 10.1007/s11705-015-1460-3.
 35. Dell, S. S., The Crystal Structure of Sodium Dodecylsulfate. *Acta Chem. Scand. A* **1977**, 31 (10), DOI 10.1107/s010827018709382x.
 36. Coiro, V. M.; Mazza, F.; Pochetti, G., Crystal phases obtained from aqueous solutions of sodium dodecyl sulfate. The structure of a monoclinic phase of sodium dodecyl sulfate hemihydrate. *Acta Crystallogr. Sect. A* **1986**, 42 (8), 991-995, DOI 10.1107/s0108270186093757.

37. Coiro, V. M.; Manigrasso, M.; Mazza, F.; Pochetti, G., Structure of a triclinic phase of sodium dodecyl sulfate monohydrate. A comparison with other sodium dodecyl sulfate crystal phases. *Acta Crystallogr. Sect. C* **1987**, 43 (5), 850-854, DOI 10.1107/S010827018709382X.
38. Callahan, J. C.; Cleary, G. W.; Elefant, M.; Kaplan, G.; Kensler, T.; Nash, R. A., Equilibrium Moisture Content of Pharmaceutical Excipients. *Drug Dev. Ind. Pharm.* **1982**, 8 (3), 355-369, DOI 10.3109/03639048209022105.
39. Council-of-Europe, *European Pharmacopoeia*, 5th Edition. Council of Europe: 2004.
40. Newman, A. W.; Reutzel-Edens, S. M.; Zografí, G., Characterization of the "hygroscopic" properties of active pharmaceutical ingredients. *J. Pharm. Sci* **2008**, 97 (3), 1047-1059, DOI 10.1002/jps.21033.
41. Bryan, W. P., Sorption hysteresis and the laws of thermodynamics. *Journal of Chemical Education* **1987**, 64 (3), 209, DOI 10.1021/ed064p209.
42. Everett, D. H., *The Solid-Gas Interface Vol. 2*. Flood, E. A., Ed. Marcel Dekker: 1967.
43. Ralston, A. W.; Hoerr, C. W., The Solubilities of the Normal Saturated Fatty Acids. *J. Org. Chem.* **1942**, 07 (6), 546-555, DOI 10.1021/jo01200a013.
44. Hoerr, C. W.; Balston, A. W., The Solubilities of the Normal Saturated Fatty Acids. II. *J. Org. Chem.* **1944**, 09 (4), 329-337, DOI 10.1021/jo01186a005.
45. Ulrich, J.; Strege, C., Some aspects of the importance of metastable zone width and nucleation in industrial crystallizers. *J. Cryst. Growth* **2002**, 237, 2130-2135, DOI 10.1016/S0022-0248(01)02284-9.
46. Kashchiev, D.; van Rosmalen, G. M., Review: Nucleation in solutions revisited. *Cryst. Res. Technol.* **2003**, 38 (7-8), 555-574, DOI 10.1002/crat.200310070.
47. Khan, S.; Ma, C. Y.; Mahmud, T.; Penchev, R. Y.; Roberts, K. J.; Morris, J.; Özkan, L.; White, G.; Grieve, B.; Hall, A.; Buser, P.; Gibson, N.; Keller, P.; Shuttleworth, P.; Price, C. J., In-Process Monitoring and Control of Supersaturation in Seeded Batch Cooling Crystallisation of L-Glutamic Acid: From Laboratory to Industrial Pilot Plant. *Org. Process Res. Dev.* **2011**, 15 (3), 540-555, DOI 10.1021/op100223a.
48. Miyata, I.; Takada, A.; Yonese, M.; Kishimoto, H., Solution Behavior of Sodium Dodecyl Sulfate in Methanol. *Bull. Chem. Soc. Jpn.* **1990**, 63 (12), 3502-3507, DOI 10.1246/bcsj.63.3502.
49. Mysels, K. J., Surface tension of solutions of pure sodium dodecyl sulfate. *Langmuir* **1986**, 2 (4), 423-428, DOI 10.1021/la00070a008.
50. Lin, S.; Lin, Y.; Chen, E.; Hsu, C.; Kwan, C., A Study of the Equilibrium Surface Tension and the Critical Micelle Concentration of Mixed Surfactant Solutions. *Langmuir* **1999**, 15 (13), 4370-4376, DOI 10.1021/la981149f.
51. Chatterjee, A.; Moulik, S. P.; Sanyal, S. K.; Mishra, B. K.; Puri, P. M., Thermodynamics of Micelle Formation of Ionic Surfactants: A Critical Assessment for Sodium Dodecyl Sulfate, Cetyl Pyridinium Chloride and Dioctyl Sulfosuccinate (Na Salt) by Microcalorimetric, Conductometric, and Tensiometric Measurements. *J. Phys. Chem. B* **2001**, 105 (51), 12823-12831, DOI 10.1021/jp0123029.
52. Hernáinz, F.; Caro, A., Variation of surface tension in aqueous solutions of sodium dodecyl sulfate in the flotation bath. *Colloids Surf. A* **2002**, 196 (1), 19-24, DOI 10.1016/S0927-7757(01)00575-1.
53. Yonekura, R.; Grinstaff, M. W., The effects of counterion composition on the rheological and conductive properties of mono- and diphosphonium ionic liquids. *Phys. Chem. Chem. Phys.* **2014**, 16 (38), 20608-20617, DOI 10.1039/c4cp02594f.
54. Cahn, A.; Haass, R. A.; Lamberti, V. Preparation of sulfonated fatty acid ester surface-active agents. 3,320,292 1967.
55. Nagy, Z. K.; Chew, J. W.; Fujiwara, M.; Braatz, R. D., Comparative performance of concentration and temperature controlled batch crystallizations. *J. Process Control* **2008**, 18 (3), 399-407, DOI 10.1016/j.procont.2007.10.006.

Graphical Abstract



Synopsis

A popular, bio-renewably sourced surfactant has been synthesized without catalyst, solvents or chlorine, with a detailed analysis on its commercial purification and material properties.